JOURNAL OF SOLID STATE CHEMISTRY 20, 397–407 (1977)

The Ordered Dispersal of Point Defects over Cubic Lattices: Application to Fluorite-Related Structures

T. C. PARKS AND W. W. BARKER

Division of Mineralogy, CSIRO, Private Bag, P.O. Wembley, Western Australia, 6014

Received May 5, 1975; in revised form December 11, 1976

Superlattices, formed by ordering one kind of defect among the sites of a cubic lattice, may be generated by the repetition of an octahedral unit which has a defect at its center and six more defects at its vertices. The superlattices are severely restricted in number by requiring the vertices of the unit to be equidistant from the center at a radius, R, and mutually separated by at least the same distance, R. Such a restriction applies to cation superlattices in pyrochlores, type-C sesquioxides, and UY_6O_{12}, and to the formal anion vacancies which relate UY_6O_{12} to fluorite. At each value of R, several superlattices may be possible, involving different fractions, $1/n$, of the cubic sites, and these are catalogued for R values less than $(14)^{1/2}a_A$ (where a_A is the cell edge of the cubic lattice). Parallel defect-rich rows may occur for the highest values of $1/n$ at a given R, but in most cases the restriction disperses defects efficiently, i.e., tends to satisfy repulsions between defects, as is demonstrated by computed electrostatic potentials. The stability of such ordered dispersals of defects (relative to their randomized alternatives) decreases as n increases, except where an increment in n involves an increase in R. Variations in the stability of superlattice phases in PrO_x may be of this type. Site potentials in the superlattices are related empirically to $n^{1/3}$ using reduced variables involving R. High symmetry is not essential to the efficient dispersal of point defects.

Introduction

Complicated crystal structures may sometimes be related to a simpler structure by the superlattice ordering of defects (vacant sites, interstitial atoms and/or substituted ions). Thus, the pyrochlore $A_2B_2O_7$ type and the type-C sesquioxides can be formally derived from the cubic fluorite structure by the ordering of vacant anion sites. These particular fluorite-related structures retain cubic symmetry (albeit with a doubled cell edge), but high symmetry is not essential to the stability of superlattices based on a cubic lattice; this is demonstrated (Fig. 1) by the homologous fluorite-related oxides Pr_nO_{2n-2} ($n = 7, 9, 10, 11, 12$) which are either triclinic or monoclinic for $n \geqslant 9$ (*1*). For $n \geqslant 9$, the location of anion vacancies within the unit cells is not known because of technical and experimental difficulties, but there is an apparent family relationship among the homologs (*2*) and at high temperatures the same composition range is spanned by the continuous α-phase in which anion vacancies are randomized. Ordering among cation sites, if present, is expected to be of secondary importance only, and the system is therefore regarded as a paradigm in the study of superlattice ordering among the sites of a cubic lattice: In the absence of a symmetry requirement, what distinguishes the observed superlattice structures from the many which are possible at each composition?

Predictions of the location of "vacancies" in Pr_nO_{2n-2} ($n \geqslant 9$) have been further prompted by their utility as models in trial-and-error structure determinations. The usual approach (*1–3*) is to arrange the vacancies in the same planes, rows, or rows of pairs, which are then spaced differently for the various homologues. Such thinking is stimulated by the success of the crystallographic shear concept which

ISSN 0022-4596

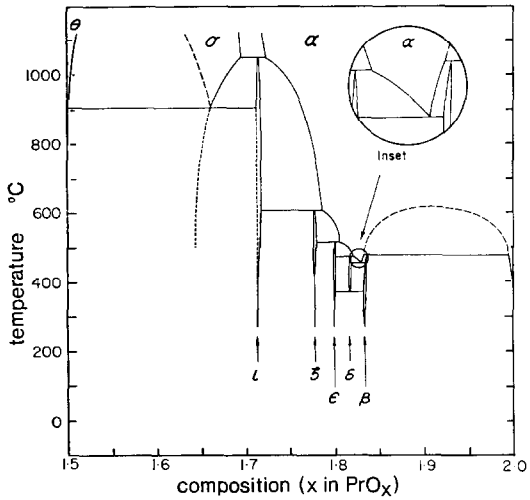

FIG. 1. The condensed phase diagram for $PrO_{1.5}$–PrO_2 (2). Single phase regions are labelled by Greek characters; two-phase regions are unlabelled. ——, assumed phase boundaries; ....., metastable phase boundaries.

applies to reduced transition metal oxides; moreover, appropriate planes or rows, etc., may be perceived (indeed, are inevitable) in the more anion-deficient fluorite-related structures such as Pr_7O_{12} and the type-C sesquioxides. Viewed differently, these hypotheses assume the persistence, over a range of concentrations of defects, of the one or two superlattice vectors which define the particular defect aggregate. This paper examines alternative hypotheses which are concerned, instead, with the *relative* sizes of *several* of the shortest superlattice vectors.

Anion vacancies are virtual positive charges in the "continuum" of the fluorite structure, and therefore repel one another. At low vacancy concentrations, one- and two-dimensional aggregates of vacancies would be stable only if they were conducive to the remaining anions relaxing from their ideal fluorite positions in order to be more closely coordinated with the cations. We demonstrate that the effect of such repulsions may be minimized without relaxation, in the alternative structures which are selected by consideration of the relative sizes of the several shortest superlattice vectors. In other words, this alternative type of rule can ensure that defects are efficiently dispersed, regardless of their concentration.

Because the stabilizing effect of such alternative rules does not rely on the relaxation of the structure around the defects, it is also independent of the positions of cations relative to anions in the parent structure. Hence the rules we propose could apply to superlattices formed in any crystal in which cations and anions each lie in cubic arrays. Anion-deficient fluorites are the particular examples chosen to illustrate the rules in this paper.

Constructing and Cataloging the Superlattices

A lattice is characterized by a basic unit from which it may be generated by endless repetition in space. The smallest such unit is the reduced cell (*4*, *5*), a parallelepiped with a lattice site at each corner and with edges which are the three shortest non-coplanar vectors of the lattice. An alternative unit is the crystallographic unit cell, which may be several times larger than the reduced cell but has the full symmetry of the lattice. For selecting defect superlattices, we refer to a third alternative, viz an octahedral unit with a defect at its center and six defects at the vertices; the complete superlattice of defects is generated by repeating the octahedron in space so that neighboring octahedra share edges as in Fig. 2 where the octahedron with center at *A* shares edges with those centered on *C* and *C'*. Although some superlattice sites are imagined

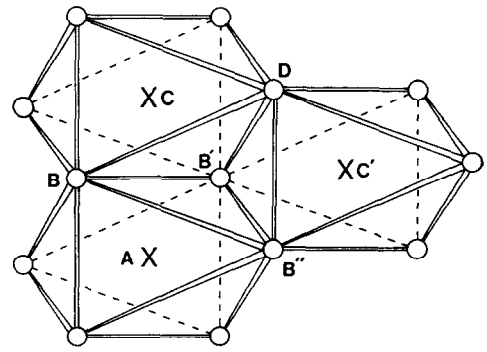

FIG. 2. Three adjoining octahedral units of a superlattice. Crosses at *A*, *C*, and *C'* are superlattice sites at centers of octahedra; remaining sites marked by circles are vertices.

as centers and some as vertices, they are all equivalent. If the superlattice is one in which each defect is coordinated by more than six defects, the shell of nearest neighbors is completed by some of the centers and/or vertices of adjacent octahedra in the lattice, the shapes of the octahedral units being compressed in one direction so that these defects are sufficiently close.

The octahedral unit and the reduced cell are related simply. The vectors which join the center to the vertices of the octahedral unit, when taken in the appropriate sense and sequence, are the parameters **a**, **b** and **c** of the reduced cell. Correspondingly, the four pairs of triangles bounded by the face diagonals of the reduced cell are equivalent to the faces of the octahedral unit. Although the stack of octahedra accounts for all the sites of a superlattice it does not fill all the space between them (unlike a stacking of reduced cells or unit cells); tetrahedra such as $BB'B''D$ remain. Hence, if a superlattice comprises $1/n$th of the sites of a cubic lattice (cell edge a_A) the octahedral units will each have a volume $4na_A^3/3$, while the reduced cell has the volume na_A^3.

We propose the restriction that the vertices of the octahedral unit should be equidistant from its center, at a separation denoted by R, and also that the vertices should be mutually separated by at least R. Such a restriction applies to the anion vacancies which relate UY_6O_{12} (and Pr_7O_{12}) to fluorite; if the unit cell edge of the anion sublattice is a_A (half the fluorite cell edge, a_F) then $R = 5^{1/2}a_A$ and the octahedral unit has the shape (I) in Fig. 3. In the same compound, the lattice of the six-coordinated U^{6+} cations (which are cation "defects" relative to fluorite) is generated by the octahedral unit II in Fig. 4, with $R = 6^{1/2}a_A$. Further octahedral units, to be described below, apply to other fluorite-related superlattices:

(i) The face-centered cubic lattice of the small, six-coordinated B cations in the pyrochlore type $A_2B_2O_7$ ($R = 8^{1/2}a_A$).

(ii) The simple cubic lattice formed by the more regularly coordinated cations in the type-C sesquioxides ($R = 2a_A$). (Note, however, that the unit cell must be further multiplied for the total structure, to describe positional relaxations of other ions.)

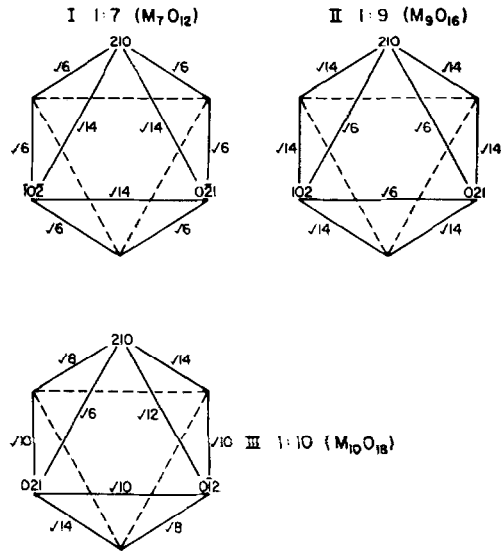

FIG. 3. Diagrammatic illustration of the three octahedral shapes in which vertices are selected from cubic lattice sites lying on a sphere centered at 0, 0, 0 with a radius of $5^{1/2}a_A$, so that vertices are at least $5^{1/2}a_A$ apart. The broken lines indicate hidden edges for which lengths are not shown. In each case, only one of the possible choices of coordinates for vertices is shown, but no other shapes are possible. Also shown is the proportion of lattice sites involved in the superlattice which is generated by repeating the octahedron in space; the oxide formula shown would arise from a similar superlattice of anion vacancies in the fluorite structure.

(iii) The rhombohedral lattice of six-coordinated cations in $Zr_{10}Sc_4O_{26}$ (6) for which $R = (10)^{1/2}a_A$.

Table I is an exhaustive catalog of superlattices possible for $3^{1/2}a_A \leqslant R \leqslant (13)^{1/2}a_A$. Since the vertices of the corresponding octahedral units must be selected from the parent cubic array, the shapes of the octahedra are severely restricted in number for each choice of R. For example, a sphere of radius $5^{1/2}a_A$, centered on the lattice site chosen as the origin, intersects 24 other lattice sites given by the permutations of the coordinates (2, 1, 0) and their negatives. These sites may be selected to

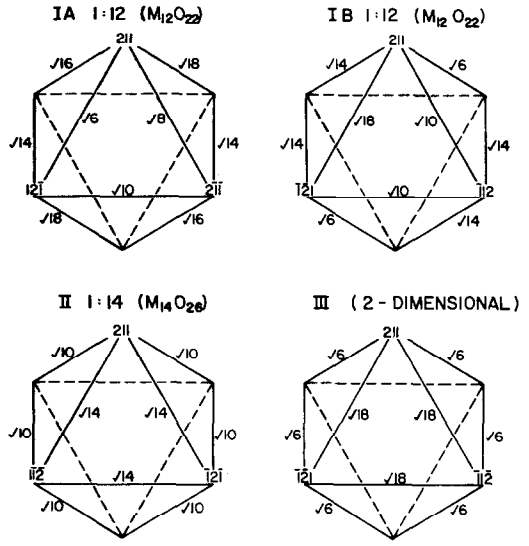

FIG. 4. The four octahedral shapes in which vertices are selected from cubic lattice sites lying on a sphere of radius $6^{1/2}a_A$ and at least $6^{1/2}a_A$ apart, shown diagrammatically as in Fig. 3. Octahedra IA and IB generate the same superlattice. Octahedron III is really a hexagon, generating a two-dimensional superlattice.

give the octahedral shapes depicted diagrammatically in Fig. 3. Because of centrosymmetry, the coordinates of only three of the six sites need be specified. Other, equivalent, choices of sites may give the same octahedral shapes, but no other shapes are possible for $R = 5^{1/2}a_A$. As a further result of centrosymmetry, any octahedron must contain three rectangular midplanes, each with a diagonal of length $2R$; hence, if one edge of the midplane has a length Q, the other has a length of $(4R^2 - Q^2)^{1/2}$. The proportions of only one triangular face on an octahedron need therefore be specified and the remaining edge lengths can be quickly written down. Since we require vertices to be separated by a distance of at least R, no edge can be less than R or greater than $3^{1/2}R$ in length. The anion sites on the sphere need only to be examined in three's to see if they form an acceptable face for an octahedron under these conditions. The allowed triangles then group themselves according to the octahedra in which they occur as faces, with no triangle occurring in more than one octahedral shape for a given value of R. When the procedure is computerized, the triangles and their sides are easily sorted by size so that the smallest faces (for example) may be used to characterize and enumerate the octahedral shapes. Note, however, that for some octahedral shapes an edge may take more than one vector form, e.g., a length of $(18)^{1/2}a_A$ may arise in a $\langle 330\rangle_A$ direction or a $\langle 114\rangle_A$ direction (where the subscript A refers the direction to the parent cubic lattice); these directions correspond to different orientations of the octahedron (and generated superlattice) relative to the anion lattice, giving rise to different symmetries for the total structure (superlattice plus fundamental lattice) and therefore requiring separate entries in the catalog, Table I. For superlattices with a coordination number greater than six, two or more alternative shapes may be possible for the octahedral unit, and in such cases Table I records all possible shapes, e.g., superlattice I for $R = 6^{1/2}a_A$ is generated by either octahedron IA or IB.

The method of construction does not preclude the octahedral unit from having one pair of faces, say $BB'B''$ in Fig. 2, so large that the associated vector AD is less than R in length. The Bravais condition then requires the vector AD to be repeated endlessly, creating vacancy-rich rows in one direction. Apart from the close approach within rows, a defect's nearest neighbor defects will be six in number in adjacent rows at a separation R. Thus, the octahedron I for $R = 5^{1/2}a_A$ generates parallel rows of defects within which defects are separated by $3^{1/2}a_A$ in the $[1\bar{1}\bar{1}]_A$ direction, as observed for the anion vacancies in the UY_6O_{12} structure type. To detect such separations shorter than R, the appropriate vectors must be calculated by adding the basic vectors contained within the octahedral unit.

The cataloging procedure also selects the various two-dimensional hexagonal superlattices which can be formed on a $\{111\}_A$ plane of the cubic lattice, i.e., the octahedral unit has degenerated to a hexagon of six defects with an additional defect at its center. These are included in Table I as the last entry for the R values at which they occur, e.g., octahedron III for $R = 6^{1/2}a_A$ and octahedron II for $R = 8^{1/2}a_A$.

TABLE I

DEFECT SUPERLATTICES GENERATED FROM OCTAHEDRAL UNITS (CIRCUMRADIUS R), IN A CUBIC LATTICE (CELL EDGE a_A)

R/a_A	Ref. No.	Edge lengths on one face of octahedron[a]	Cross reference for faces[c]	Remarks on octahedron and generated superlattice[a,b]	n[d]	ϕ[e]
$\sqrt{3}$		$\sqrt{8}$: $\sqrt{8}$: $\sqrt{8}$	A	B.c.c. superlattice of defects, $a_S = 2a_A$	4	.72785
2		$\sqrt{8}$: $\sqrt{8}$: $\sqrt{8}$	A	Simple cubic superlattice of defects, $a_S = 2a_A$	8	.56746
$\sqrt{5}$	(I)	$\sqrt{14}$:$\sqrt{14}$:$\sqrt{14}$	B	Defects aggregate to a $[111]_A$ separation within parallel rows	7	.59541
	(II)	$\sqrt{6}$: $\sqrt{6}$: $\sqrt{6}$		6 nearest neighbours at $\sqrt{5}$, 6 next-nearest at $\sqrt{6}$, 6 at $\sqrt{11}$, etc.	9	.55411
	(III)	$\sqrt{6}$: $\sqrt{8}$:$\sqrt{10}$	C	6 nearest neighbours at $\sqrt{5}$, 2 next-nearest at $\sqrt{6}$, 2 at $\sqrt{8}$, etc.	10	.53154
$\sqrt{6}$	(IA)	$\sqrt{6}$: $\sqrt{8}$:$\sqrt{10}$	C(+E)	Equivalent; each octahedron generates the same superlattice;	12	.50188
	(IB)	$\sqrt{10}$:$\sqrt{10}$:$\sqrt{18}$	D	8 nearest neighbours at $\sqrt{6}$, 2 next-nearest at $\sqrt{8}$, 4 at $\sqrt{10}$, etc.		
	(II)	$\sqrt{14}$:$\sqrt{14}$:$\sqrt{14}$	B	6 nearest neighbours at $\sqrt{6}$, 6 next-nearest at $\sqrt{10}$, 2 at $\sqrt{12}$, etc.	14	.47350
	(III)	$\sqrt{18}$:$\sqrt{18}$:$\sqrt{18}$	Fc	Octahedron degenerates to a hexagon, generating a 2-D lattice		
$\sqrt{8}$	(IA)	$\sqrt{8}$: $\sqrt{8}$: $\sqrt{8}$	A	Equivalent; each octahedron generates a f.c.c. superlattice of	16	.45849
	(IB)	$\sqrt{16}$:$\sqrt{24}$:$\sqrt{24}$	H	defects, $a_S = 4a_A$		
	(II)	$\sqrt{24}$:$\sqrt{24}$:$\sqrt{24}$	G	Octahedron degenerates to a hexagon, generating a 2-D lattice		
3[f]	(I)	$\sqrt{26}$:$\sqrt{26}$:$\sqrt{26}$	I	Defects aggregate to a $[111]_A$ separation within parallel rows	13	.45199
	(II)	$\sqrt{10}$:$\sqrt{10}$:$\sqrt{20}$		8 nearest neighbours at $\sqrt{9}$, 4 next-nearest at $\sqrt{10}$, 2 at $\sqrt{16}$, etc.	20	.42559
	(III)	$\sqrt{10}$:$\sqrt{10}$:$\sqrt{18}$	D	6 nearest neighbours at $\sqrt{9}$, 4 next-nearest at $\sqrt{10}$, 2 at $\sqrt{11}$, etc.	21	.41828
	(IV)	$\sqrt{10}$:$\sqrt{16}$:$\sqrt{18}$	E(+J)	6 nearest neighbours at $\sqrt{9}$, 2 next-nearest at $\sqrt{10}$, 2 at $\sqrt{16}$, etc.	24	.39646
	(V)	$\sqrt{18}$:$\sqrt{18}$:$\sqrt{18}$	Ft	Simple cubic superlattice rotated relative to normal lattice; total structure has tetrahedral symmetry. $a_S = 3a_A$.	27	.37831
	(VI)	$\sqrt{18}$:$\sqrt{18}$:$\sqrt{18}$	Fc	Simple cubic superlattice parallel to normal lattice. $a_S = 3a_A$	27	.37831
	(VII)	$\sqrt{12}$:$\sqrt{20}$:$\sqrt{24}$	K(+H)	6 nearest neighbours at $\sqrt{9}$, 4 next-nearest at $\sqrt{12}$, 2 at $\sqrt{16}$, etc.	24	.39749
$\sqrt{10}$	(I)	$\sqrt{26}$:$\sqrt{26}$:$\sqrt{26}$	I	6 nearest neighbours at $\sqrt{10}$, 2 next-nearest at $\sqrt{12}$, 6 at $\sqrt{14}$, etc.	26	.38950
	(II)	$\sqrt{14}$:$\sqrt{14}$:$\sqrt{14}$	B	6 nearest neighbours at $\sqrt{10}$, 6 next-nearest at $\sqrt{14}$, 6 at $\sqrt{24}$, etc.	28	.37774
	(III)	$\sqrt{18}$:$\sqrt{20}$:$\sqrt{26}$	J(+N)	6 nearest neighbours at $\sqrt{10}$, 2 next-nearest at $\sqrt{14}$, 2 at $\sqrt{18}$, etc.	30	.36708
$\sqrt{11}$	(I)	$\sqrt{32}$:$\sqrt{32}$:$\sqrt{32}$	L	Defects aggregate to a $[111]_A$ separation within parallel rows	16	.40402
	(II)	$\sqrt{12}$:$\sqrt{20}$:$\sqrt{24}$	K	6 nearest neighbours at $\sqrt{11}$, 2 next-nearest at $\sqrt{12}$, 2 at $\sqrt{19}$, etc.	32	.36055
	(III)	$\sqrt{24}$:$\sqrt{24}$:$\sqrt{24}$	G	6 nearest neighbours at $\sqrt{11}$, 6 next-nearest at $\sqrt{20}$, 6 at $\sqrt{24}$, etc.	36	.34425
$\sqrt{12}$		$\sqrt{32}$:$\sqrt{32}$:$\sqrt{32}$	L	B.c.c. distribution of defects, $a_S = 4a_A$	32	.36392
$\sqrt{13}$	(I)	$\sqrt{38}$:$\sqrt{38}$:$\sqrt{38}$	M	Defects aggregate to a $[111]_A$ separation within parallel rows	19	.36433
	(II)	$\sqrt{14}$:$\sqrt{16}$:$\sqrt{38}$	P	Defects aggregate to a $[210]_A$ separation within parallel rows	24	.37748
	(III)	$\sqrt{14}$:$\sqrt{14}$:$\sqrt{14}$	B	6 nearest neighbours at $\sqrt{13}$, 6 next-nearest at $\sqrt{14}$, 6 at $\sqrt{27}$, etc.	35	.35305
	(IV)	$\sqrt{18}$:$\sqrt{18}$:$\sqrt{36}$		8 nearest neighbours at $\sqrt{13}$, 2 next-nearest at $\sqrt{16}$, 4 at $\sqrt{18}$, etc.	36	.34988
	(V)	$\sqrt{14}$:$\sqrt{14}$:$\sqrt{16}$		6 nearest neighbours at $\sqrt{13}$, 4 next-nearest at $\sqrt{14}$, 2 at $\sqrt{16}$, etc.	36	.34947
	(VI)	$\sqrt{14}$:$\sqrt{18}$:$\sqrt{26}$	Q	6 nearest neighbours at $\sqrt{13}$, 2 next-nearest at $\sqrt{14}$, 2 at $\sqrt{18}$, etc.	39	.33905
$\sqrt{14}$	(I)	$\sqrt{14}$:$\sqrt{16}$:$\sqrt{38}$	P	Defects aggregate to a $[211]_A$ separation within parallel rows	28	.36400
	(II)	$\sqrt{38}$:$\sqrt{38}$:$\sqrt{38}$	M	Defects aggregate to a $[222]_A$ separation within parallel rows	38	.34328
	(III)	$\sqrt{20}$:$\sqrt{20}$:$\sqrt{40}$		8 nearest neighbours at $\sqrt{14}$, 2 next-nearest at $\sqrt{16}$, 4 at $\sqrt{20}$, etc.	40	.33771
	(IVA)	$\sqrt{14}$:$\sqrt{18}$:$\sqrt{20}$	N	Equivalent; each octahedron generates the same superlattice,	42	.33101
	(IVB)	$\sqrt{14}$:$\sqrt{20}$:$\sqrt{30}$		in which separations of $\sqrt{18}$ are $(330)_A$ vectors;		
	(IVC)	$\sqrt{14}$:$\sqrt{18}$:$\sqrt{26}$	Q	8 nearest neighbours at $\sqrt{14}$, 2 next-nearest at $\sqrt{18}$, 2 at $\sqrt{20}$, etc.		
	(VA)	$\sqrt{14}$:$\sqrt{18}$:$\sqrt{20}$		Equivalent; each octahedron generates the same superlattice,	42	.33101
	(VB)	$\sqrt{14}$:$\sqrt{20}$:$\sqrt{30}$		in which separations of $\sqrt{18}$ are $(411)_A$ vectors;		
	(VC)	$\sqrt{14}$:$\sqrt{18}$:$\sqrt{26}$		8 nearest neighbours at $\sqrt{14}$, 2 next-nearest at $\sqrt{18}$, 2 at $\sqrt{20}$, etc.		
		(plus five other superlattices, for n = 44, 46, 48, 50 and 52).				
	(XI)	$\sqrt{42}$:$\sqrt{42}$:$\sqrt{42}$		Octahedron degenerates to hexagon, generating a 2-D lattice		

[a] All coordinates and directions are referred to the fundamental cubic lattice. All distances and vectors are divided by a_A.

[b] Parameters of cubic superlattices are denoted by a_S.

[c] Letters in parentheses refer to a face other than the one explicitly listed in that row of the Table. (See text on "Intergrowth").

[d] $1/n$ is the fraction of fundamental sites which are defective. M_nO_{2n-2} is the formula of a fluorite-type oxide with $1/n$ anion sites vacant.

[e] ϕ $(e/\text{Å})$ is the electrostatic potential at a superlattice site, due to negative charges e at the other superlattice sites, immersed in a neutralizing continuum, assuming a_A = 2.5Å.

[f] For $R = 3a_A$, octahedra I to V involve permutations of the coordinates 2,2,1 only, octahedron VI involves permutations of 3,0,0 only, and octahedron VII involves sites of both types.

Relative Stability of Superlattices

Brunner (7) has enlarged on the fact that lattices which achieve the closest packings of spheres also involve the highest coordinations of spheres by spheres, and are the same lattices which achieve the widest sepatations between (i.e., dispersal of) points confined in a given volume. It is usually supposed that cubic or hexagonal symmetry is a necessary feature of such lattices, but computations of coulombic repulsions for the superlattices in

Table I refute this; *regardless of symmetry* an arrangement which coordinates each defect with an abundance of neighboring defects is a more efficient dispersal of defects than other arrangements in which defects have fewer (and therefore closer) nearest neighbors. Similar comments apply to next-nearest neighbors and successive shells of neighbors.

In most cases the "octahedron rule" places a lower limit of six on the coordination of defects by defects and therefore places a lower limit on the efficiency with which the defects are dispersed. The exceptions are the superlattices which contain parallel, defect-rich rows, as noted in Table I, and even in these structures the rule acts to achieve wide separations between defects in adjacent rows.

The simplest comparison between superlattices is made by ignoring the normal sites and imagining each superlattice site to be occupied by a point charge $-e$ (equivalent to one electron) immersed in a continuum of neutralizing positive charge. The Ewald method (*8*) enables the potential to be computed at any position within such a lattice and Table I lists the potential ϕ at the actual superlattice sites, assuming $a_A =$ 2.5 Å.

For each negative charge, e, ϕ is positive because the neutralizing continuum is a stable environment only partly counteracted by the presence of the other superlattice points (depending on how well they are dispersed). There is a tendency for ϕ to decrease as the defect concentration decreases, i.e., as the volume, na_A^3, per superlattice site increases and the neutralizing continuum becomes attenuated. However, there is a disproportionately large decrease in ϕ between superlattice I for $R/a_A = 5^{1/2}$ $(n = 7)$ and the simple cubic superlattice at $R/a_A = 2$ $(n = 8)$. This indicates that the former superlattice disperses defects more efficiently than the simple cubic superlattice, and shows that the aggregation of defects to a separation of $3^{1/2}a_A$ within $[1\bar{1}\bar{1}]$ rows is more than offset by spreading an abundance of next-nearest defects at $5^{1/2}a_A$ and $6^{1/2}a_A$ (six at each of these separations).

To provide a more sensitive comparison of the efficiency of dispersal, ϕ needs to be compensated against the general decrease which it suffers as n increases (i.e., as the concentration of defects decreases). Since potentials are inversely proportional to distance, the ϕ for all superlattices obeying the "octahedron rule" may be brought to the same scale by multiplying by the appropriate value of R. The fraction, $1/n$, of cubic sites involved in the superlattice, may be similarly scaled by multiplying by R^3. Thus, the simple cubic superlattices for $R = 3a_A$ (entries V and VI in Table I) provide the same values of the reduced variables $\phi \cdot R$ and R^3/n as does the simple cubic superlattice for $R = 2a_A$. If the few superlattices containing linear aggregates are excluded, a graph of $\phi \cdot R$ versus $n^{1/3}/R$ (Fig 5) shows that the remaining superlattices plot close to a straight line between the points for face-centered (FCC) and simple-cubic (SC) superlattices. The FCC and SC lattices therefore represent upper and lower limits to the efficiency with which the "octahedron rule" disperses defects. However, with the exception of body-centered-cubic superlattices, the intermediate points in Fig. 5 represent symmetries ranging from rhombohedral to monoclinic which can be determined by applying Niggli's tables (*4*, *5*) to the shapes of the reduced cells. Note that the *overall* symmetry might be reduced to triclinic when the superlattices are superimposed on ionic crystal structures such as fluorite.

The good fit to a straight line shown in Fig. 5 suggests an empirical relationship between ϕ and the volume and edge lengths of the reduced cell for Bravais lattices which have a coordination number of six or more. This is the subject of a separate study to be published by one of us (T.C.P.), and Fig. 5 is captioned in these more general terms.

We have drawn a distinction between two ways in which superlattice ordering may stabilize point defects in ionic crystals, viz by dispersing defects and by facilitating the relaxation of cations towards anions. It is possible that the "octahedron rule" favors relaxation also, but we have not examined this prospect. However, the relative importance of defect dispersal may be gauged from the potential ψ_0 at ordered, vacant anion sites in, for example, the fluorite structure.

For crystals consisting of several superposed

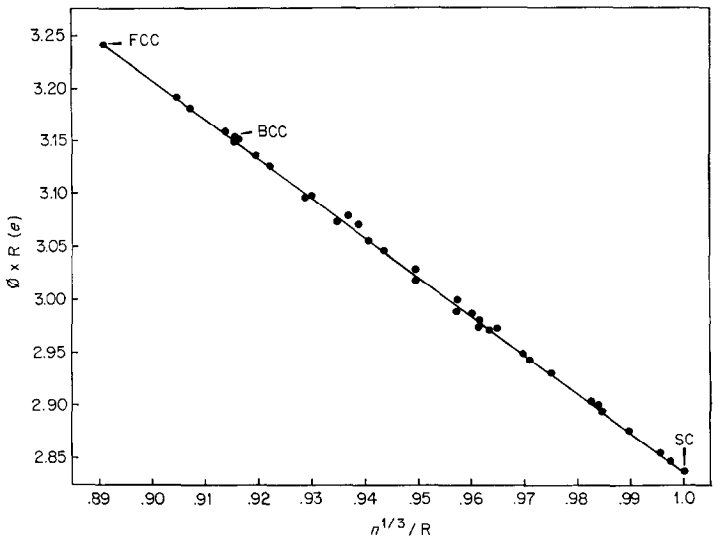

FIG. 5. The "reduced site potential," $\phi \cdot R$ for Bravais lattices in which the coordination number is at least six. ϕ (e/Å) is the site potential when each lattice site has the electronic charge $-e$, immersed in a continuum of neutralizing charge. R (Å) is the separation between nearest neighbors and n (Å^3) is the volume per site. Arrows indicate the points for face-centered (FCC), body-centered (BCC) and simple-cubic (SC) symmetry. The points plotted relate to superlattices obtained by selecting $1/n$th of the sites of a cubic lattice, cell edge 2.5 Å.

ionic lattices, the potential at a site is obtained by summing the potentials which the Ewald method produces from each constituent lattice. (The effects of the neutralizing continuums cancel, provided the total structure is neutral.) When the superlattices of Table I are applied, without relaxation, to anion-deficient fluorite-type oxides of cell edge 5 Å,

$$\psi_0 = 0.6415488(1/n - 1) + 2.269838 - 2\phi,$$

where the first term in the sum is due to the cations, the second is the contribution that would result from a complete lattice of oxide ions, and 2ϕ arises from the missing anions.

ψ_0 has reciprocity relationships (*9*) with the potentials at the cation sites and remaining anions, so that the effect of vacancy ordering on the Madelung energy is totally reflected in the difference between ψ_0 and ψ_R, the average anion site potential when vacancies are randomized. Despite claims to the contrary (*10*), ψ_R is given by the "partial occupancy" model (*11*) so that $\psi_R = 1.6282892\ (1 - 1/n)$.

Ideally, the potential at any vacant site should be zero. For the superlattices up to $R = 8^{1/2}a_A$, $\psi_R - \psi_0$ is greater than $\psi_R/2$, so that the dispersal of vacancies achieves better than half the complete stabilization of vacancies.

Fig. 6 is a plot of $\psi_R - \psi_0$ versus $n^{1/3}$ for the dispersed superlattices of Table I, together with the rhombohedral and hexagonal structures containing parallel "$[111]_A$ strings" of vacancies proposed by Hyde *et al.* (*2*) and the structures containing $(213)_A$ planes of $[11\bar{1}]_A$ strings proposed by Martin (*3*). The points for the "dispersed" structures fall on a series of straight line segments, each segment relating to the particular value of R/a_A with which it is labelled. These segments are arranged *en echelon* to give a slow general decrease in $\psi_R - \psi_0$ as $n^{1/3}$ increases (i.e., as the proportion of vacancies decreases). In contrast, the decrease is rapid for the "[111] string" structures and catastrophic for the "(213) plane" structures. $\psi_R - \psi_0$ eventually becomes negative for such structures, indicating that they are less stable than their randomized alternatives.

Alternative Rules for Dispersing Defects

While the octahedron rule sets a lower limit on the efficiency of the dispersal of defects, it

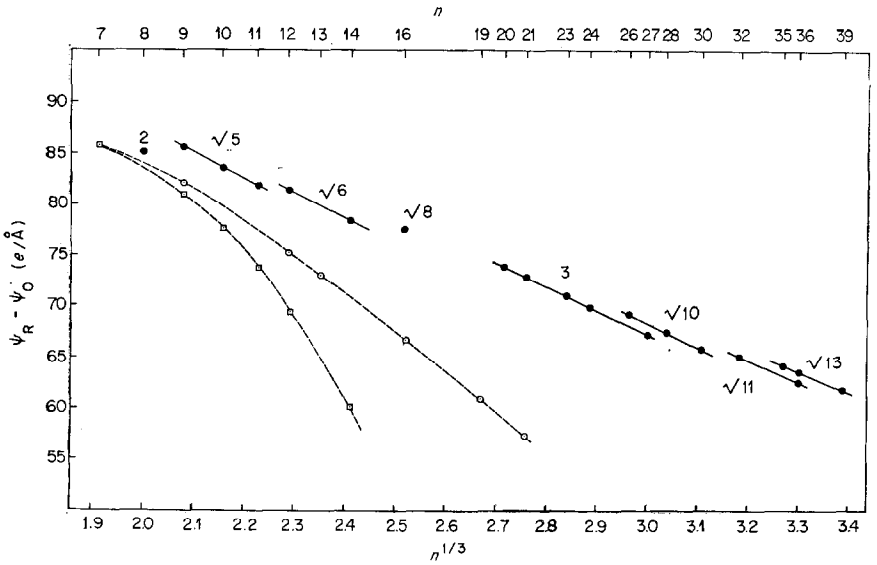

FIG. 6. The stability gained by ordering vacant anion sites in a fluorite-type oxide of 5 Å cell edge. ψ_0 is the potential at a vacant site in the ordered structure, and ψ_R is the average anion site potential in a random structure of the same composition. $1/n$ is the fraction of anion sites vacant so that M_nO_{2n-2} is the oxide formula. The ideal potential at a vacant site is zero, whereas $\psi_R = 1.6282892\ (1 - 1/n)$. The unfilled circles are for hexagonal and rhombohedral structures containing [111] "strings" of vacancies (*1*, *2*). The squares are structures containing [321] planes of vacancies after Martin (*3*). The filled circles are dispersed arrangements of vacancies, which plot on straight line segments labelled by values of $R/2.5$ where R (Å) is the closest approach between vacancies.

does not produce all the superlattices which surpass that limit. Note that for $R = (13)^{1/2}a_A$, superlattices IV and V both provide for 1/36 of the sites to be defective. These superlattices have almost identical values of ϕ, but two of the eight nearest neighbors at $(13)^{1/2}a_A$ in IV are replaced by four next-nearest at $(14)^{1/2}a_A$ in V. This suggests that a rule requiring four nearest neighbors at $k^{1/2}a_A$, plus four next-nearest, at $(k+1)^{1/2}a_A$, would disperse defects with efficiency similar to the octahedron rule.

An exhaustive search for such superlattices produced only three within the range of Table I; one for $k = 5^{1/2}$ and 1/11 sites defective, another at $k = 3$ and 1/23 sites defective, and a third at $k = (11)^{1/2}$ and 1/32 sites defective. For the first two of these $\psi_R - \psi_0$ is plotted on Fig. 6. The point for $k = (5)^{1/2}$ falls on the line for $R = 5^{1/2}a_A$, but subsequent points are increasingly displaced from the "$R = k^{1/2}a_A$ line" towards the "$R = (k+1)^{1/2}a_A$ line" (i.e., they disperse vacancies slightly better than the trend of the octahedron rule when the closest approach between vacancies is the same).

Intergrowth Between Superlattices

It frequently happens that octahedral units for differing values of R have a face of the same size and shape. This means that the corresponding superlattices, in one direction, will contain the same sort of parallel defect-rich planes, along which it is possible to match the superlattices geometrically in cases of intergrowth; the superlattices can be viewed as differing only in the spacing between these planes. A column of Table I therefore provides cross references between different octahedra which have a face in common. The two-dimensional superlattices are not without significance in this regard; they may possess some stability in their own right, and when they have geometry in common with planar networks in a three-dimensional superlattice they may be important as planes along which the three-dimensional superlattice may be terminated.

The midplanes of the octahedral units also represent defect-rich planes in the superlattice. At a given value of R, the same sort of mid-

plane usually occurs in more than one octahedral shape, and again represents a type of plane along which the corresponding superlattices can be matched. However, when midplanes are used for this purpose it frequently happens that defects on opposite sides of the plane are brought to a separation less than R (T. Parks, unpublished work).

Intergrowth would be especially favored between superlattices which are close in composition and in the values of R and ϕ, a situation which is increasingly more frequent for larger R and lower vacancy concentration. Low vacancy concentrations are also more likely to be involved in intergrowth because of the increasing occurrence of alternative superlattices for the same concentration, sometimes at the same value of R.

Rhombohedral "String" Structures

The superlattices in Table I are obtained by selecting sites from a simple cubic lattice with cell edge a_A, but where R/a_A is the square root of an even number, the superlattices may also be used as patterns for distributing defects over a face-centered cubic (FCC) lattice with a cell edge of $2a_A$. Mention has already been made of the fluorite-related structures in which six-coordinated cations are arranged according to superlattices of Table I, viz UY_6O_{12}, the pyrochlores, $Zr_{10}Sc_4O_{26}$, and the type-C sesquioxides. Of these, UY_6O_{12} (which is isostructural with ι-Pr_7O_{12} and $Zr_3Sc_4O_{12}$) is special in that the anion vacancies as well as the six-coordinated cations are arranged according to a superlattice from Table I ($R/a_A = 5^{1/2}$ and $6^{1/2}$, respectively). It is, in fact, the first member of an infinite homologous series of rhombohedral structures with the same geometrical properties, containing parallel strings of vacancies (internal spacing $a_A[1\bar{1}\bar{1}]$) and six-coordinated cations (internal spacing $a_A[2\bar{2}\bar{2}]$). Typically, the arrangement of vacancies is given by a superlattice constructed with $R/a_A = k^{1/2}$ (k odd) while the corresponding superlattice of six-coordinated cations has $R/a_A = (k+1)^{1/2}$. The octahedral units in each case are dominated by two large equilateral faces (giving rise to the rhombohedral symmetry) with edges $(3k-1)^{1/2}a_A$ long, while the oxide formula is M_nO_{2n-2} with $n = (3k-1)/2$. The idealized unit cell in the hexagonal setting has $a = (3k-1)^{1/2}a_F/2$, but the other parameter is constant at $c = 3^{1/2}a_F$. There are gaps in the series, e.g., $M_{10}O_{18}$ and $M_{22}O_{42}$ are absent because there are no oxygen lattice vectors with length $7^{1/2}a_A$ or $(15)^{1/2}a_A$, and the numerology of vectors with lengths $8^{1/2}a_A$ and $(16)^{1/2}a_A$ is such that the corresponding cation superlattices cannot be constructed either.

Besides dispersing defects efficiently, the UY_6O_{12} structure favors relaxation from ideal fluorite positions towards closer coordination between cations and remaining anions (*6*). We have not yet been able to determine whether this property is due to the coincidence of two of the superlattices of Table I. If it is, one might expect to synthesize other structures low in the series, provided that appropriate chemical substitutions were made. Higher in the series the close approach of defects within rows becomes increasingly unfavorable (relative to alternative structures in which the defects are more widely dispersed) perhaps to an extent which could not be overcome by any favorable relaxation. These prospects are the subject of a separate study (T.C.P.).

Application to the Praseodymium Oxides

Unit cell dimensions for the higher homologs Pr_9O_{16}, etc., have recently been determined by Kunzmann and Eyring (*1*) using electron diffraction, but the positions of vacancies within these cells is still unknown. Kunzmann and Eyring have proposed that vacancies are separated by $a_A[111]$ in pairs, the centers of which are strung along the $[21\bar{1}]_A$ axis, thus preserving some of the close approaches between vacancies observed in Pr_7O_{12}. It is equally valid to disperse the vacancies more widely within the unit cells, seeking agreement with the arrangements shown in Figs. 3 and 4. Before making such comparisons, it should be noted that the unit cells of the "dispersed vacancy" models may be enlarged or lowered in symmetry by subsidiary ordering of cations and relaxations from ideal sites, i.e., the experimental unit cell vectors should be vectors of the model structures, though not

necessarily the shortest vectors. Thus an encouraging agreement is seen for $Pr_{12}O_{22}$ which is observed to be monoclinic with the idealized unit cell vectors $\mathbf{a} = \frac{1}{2}a_F[21\bar{1}]$, $\mathbf{b} = \frac{1}{2}a_F[0\bar{3}\bar{3}]$, $\mathbf{c} = a_F[0\bar{2}2]$; the dispersed vacancy model is C-centered with the same **a** and **b** but only half the observed **c** vector. $Pr_{11}O_{20}$ is observed to be triclinic with $\mathbf{a} = \frac{1}{2}a_F[21\bar{1}]$, $\mathbf{b} = \frac{1}{2}a_F[\bar{1}32]$, $\mathbf{c} = \frac{1}{2}a_F[1\bar{1}2]$ which, with vacancies positioned at 0, 0, 0, and 0, $\frac{1}{2}$, $\frac{1}{2}$, is equivalent to the model structure mentioned under "Alternative Rules for Dispersing Defects." For Pr_9O_{16}, Kunzmann and Eyring found the triclinic unit cell vectors $\mathbf{a} = \frac{1}{2}a_F[21\bar{1}]$, $\mathbf{b} = \frac{1}{2}a_F[031]$, $\mathbf{c} = \frac{1}{2}a_F[1\bar{1}2]$, which cannot be matched to the rhombohedral "dispersed vacancy" model having the pseudohexagonal parameters $a = 6^{1/2}a_F/2$ and $\mathbf{c} = 3(3)^{1/2}a_F$. However, the dispersed model bears some resemblance to a high-temperature modification found earlier (*12*) with the hexagonal parameters $a = 6^{1/2}a_F/2$ and $\mathbf{c} = 3^{1/2}a_F$. The dispersed model derived for $Pr_{10}O_{18}$ using the "octahedron rule" is triclinic with $\mathbf{a} = a_F[101]$, $\mathbf{b} = \frac{1}{2}a_F[0\bar{3}1]$, $\mathbf{c} = \frac{1}{2}a_F[\bar{2}11]$, which cannot be matched to the observed triclinic structure with $\mathbf{a} = \frac{1}{2}a_F[21\bar{1}]$, $\mathbf{b} = \frac{1}{2}a_F[0\bar{5}\bar{5}]$, $\mathbf{c} = a_F[0\bar{2}2]$. However, as explained above. it may be possible to disperse defects using rules other than those described in this paper, if the emphasis on high coordination numbers is shifted to the second or subsequent shells of neighboring vacancies.

We will continue our efforts to disperse vacancies within the observed unit cells, because such structures may explain several features of the PrO_x phase diagram (Fig. 1). The most puzzling of these is the absence of a compound Pr_8O_{14}, since previous structural models (*1–3*) for the Pr_nO_{2n-2} series have provided structures at $n = 8$ which do not depart from the trends at neighboring compositions. However, vacancy superlattices obeying the "octahedron rule," for example, possess the required variation in character. Without allowing for relaxation of ions from their ideal fluorite sites, Fig. 6 shows that an oxide, M_8O_{14}, would be somewhat less favored (relative to the disordered state) than M_7O_{12} or M_9O_{16}. Instead, Fig. 5 shows that the simple cubic superlattice involved in this M_8O_{14} is the least efficient means of dispersing vacancies that can result if one requires the vacancy superlattice to have a coordination number of six or more. As mentioned above, it is occasionally possible at other compositions to find superlattices which disperse vacancies well with a coordination number less than six, but only if analogous constraints are imposed on the second and higher shells of neighboring vacancies. We could find no such alternatives at M_8O_{14}, so that the simple cubic superlattice remains the best means of dispersing vacancies at this composition but nevertheless is inferior to the structures possible at M_7O_{12} or M_9O_{16}.

At high temperatures, the broad, cubic σ- and α-solid solutions are separated by a narrow but persistent gap in miscibility, centered approximately on the Pr_7O_{12} composition. σ-PrO_x occupies the composition region where approaches of $a_A\langle 111\rangle$ between vacancies are inevitable, with the consequential presence of cations which are six-coordinated by anions. This phase is continuous with the metastable ϕ-Pr_2O_3, a type-C sesquioxide in which the "octahedron rule" applies not to the vacancies themselves but to the six-coordinated cations at the centers of vacancy pairs oriented along $\langle 111\rangle_A$. The α-phase, however, spans the region where the coordination of cations by anions need not fall below seven, if the vacancies are dispersed according to a simple geometrical restriction such as the octahedron rule. ι-Pr_7O_{12} is special in that both the anion vacancies and six-coordinated cations are dispersed according to superlattices obeying the octahedron rule. (The dispersal of vacancies arises from the abundance of second and third nearest neighbors, which outweighs the approach of $a_A[111]$ between nearest neighbor vacancies.) Could this be the reason for the prominence of ι-Pr_7O_{12} as a divide between the α and σ regions?

At low temperatures, α-PrO_x is replaced by the discrete compounds Pr_nO_{2n-2} ($n = 9$, 10, 11, 12) in a series of peritectoids. The electrostatic potentials plotted in Fig. 6 for the "dispersed" structures M_9O_{16}, $M_{10}O_{18}$, and $M_{11}O_{20}$ (which contain vacancies separated by $5^{1/2}a_A$) are in accord with the regular decrease in peritectoid temperatures observed for the praseodymium oxides of the same

composition. We suggest that the curious eutectoid in the α-phase near $Pr_{12}O_{22}$ (Fig. 1, inset) occurs because the vacancy concentration has fallen to the point where an ordered compound can form with vacancies no closer than $6^{1/2}a_A$.

Acknowledgments

We are grateful to Drs. J. Graham and A. W. Mann for their helpful discussions. A computer program EWALDPOT, based on the report by Slater and Decicco (*13*), was obtained from Dr. I. D. Campbell of the CSIRO Division of Chemical Physics.

References

1. P. KUNZMANN AND L. EYRING, *J. Solid State Chem.* **14**, 229–237 (1975).
2. B. G. HYDE, D. J. M. BEVAN, AND L. EYRING, *Phil. Trans. Roy. Soc. (London)* **A259**, 583–614 (1966).
3. R. L. MARTIN, *J. Chem. Soc. (Dalton Trans.)* 1335–1350 (1974).
4. L. V. AZAROFF AND M. J. BUERGER, "The Powder Method," Chap. 11, McGraw-Hill, New York (1958).
5. A. MIGHELL, A. SANTORO, AND J. D. H. DONNAY, *in* "International Tables for X-Ray Crystallography," Vol. I, 3rd ed., pp. 530–535, Kynoch Press, Birmingham, England (1969); See also *Acta Crystallogr.* **B29**, 309 (1973).
6. M. R. THORNBER, D. J. M. BEVAN, AND J. GRAHAM, *Acta Crystallogr.* **B24**, 1183–90 (1968).
7. G. O. BRUNNER, *Acta Crystallogr.* **A27**, 388–390 (1971).
8. M. P. TOSI, *Solid State Phys.* **16**, 1–120 (1964).
9. C. K. COOGAN, *Australian J. Chem.* **20** 2551–2565 (1967).
10. R. F. GIESE, JR., *Nature* **256**, 31–32 (1975).
11. W. W. BARKER, J. GRAHAM, AND T. P. SPEED, submitted for publication.
12. J. O. SAWYER, B. G. HYDE, AND L. EYRING, *Bull. Soc. Chim. France* 1190–1199 (1965).
13. J. C. SLATER AND P. DECICCO, in *M.I.T. Solid State Molecular Theory Group, Quqrterly Progress Report*, No. 50, p. 46, October (1963).